

1

## Supplement

### 2 **Temperature Dependencies of the Degradation of NO, NO<sub>2</sub> and HONO on a** 3 **Photocatalytic Dispersion Paint**

4

5 Daniela Pill, Peter Wiesen and Jörg Kleffmann\*

#### 6 **S1 Photocatalytic Paint**

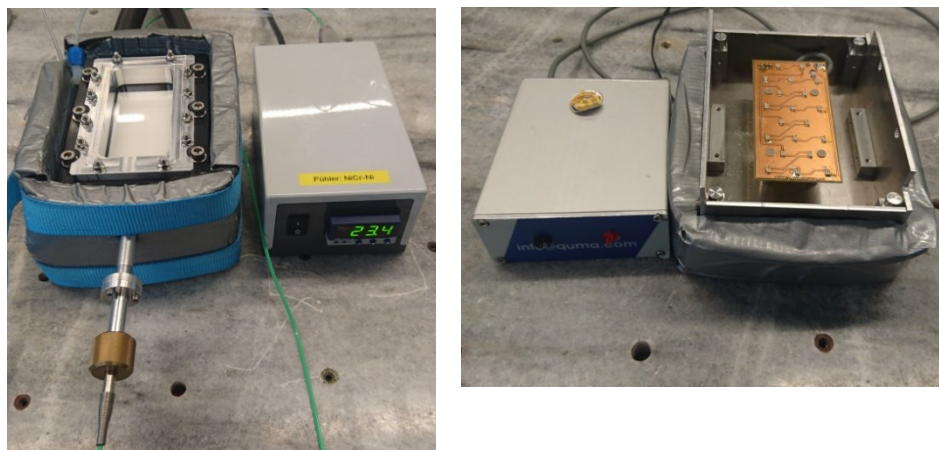
7 The used paint (StoPhotosan NO<sub>x</sub> dispersion paint, white) was already applied in a former  
8 study<sup>1</sup> and showed a high photocatalytic activity against NO, NO<sub>2</sub> and HONO. The  
9 photocatalyst used (Kronos Int.: vlp 7000) is a carbon doped titanium dioxide in Anatase  
10 modification. As specified by the manufacturer the photocatalyst displays photoactivity not  
11 only under UV but also under visible light (<500 nm). The paint is composed of an organic  
12 binder system which was optimized for low oxygenated VOC emissions<sup>2</sup> and contains a few  
13 wt % of the photocatalyst and 15 % of a non-catalytic TiO<sub>2</sub> in Rutil modification to obtain  
14 higher opacity. The pH of the paint is in the range 8 - 8.5.

15 The paint was hand-brushed on one side of a PVC (polyvinyl chloride) plate (49 mm × 99 mm  
16 × 8 mm) and the sample was already in regular use for several years in the laboratory. Before  
17 each experiment the surface was carefully washed with Millipore water, dried under nitrogen  
18 and irradiated overnight by two fluorescence tubes ( $\lambda_{max}$  = 365 nm) with an UVA irradiance of  
19 33 W m<sup>-2</sup> to decompose possible adsorbed impurities und to obtain more reproducible results.  
20

#### 21 **S2 Photoreactor**

22 The photocatalytic activity of the sample was studied in a temperature controlled flow  
23 photoreactor, which is adapted to ISO 22197-1,<sup>3</sup> see Fig. S1 and Fig. S2. As recommended by  
24 ISO, the sample bed has a dimension of 50 mm × 100 mm. However, in contrast to the ISO  
25 standard, the geometry of the reactor, the experimental conditions and the data evaluation  
26 were significantly improved, as explained in detail elsewhere.<sup>4</sup> The reactor consists of an  
27 upper cap made by PVC, which contains the inlet and exit for the gas mixture (with each 6  
28 evenly spread inlet/exit holes), the UVA transparent Pyrex glass window and a thermocouple  
29 for surface temperature measurements. The lower sample holder is made by aluminum, which  
30 contains variable spacers to adjust the distance of the sample to the Pyrex window for variable

31 sample sizes. The sample holder is temperature controlled in the range 5-60°C by flushing  
32 water through channels in the aluminum block using an external thermostat (Thermo-Haake  
33 DC10-K10). Before the gas mixture enters the reactor, it is thermally equilibrated to the  
34 reactor temperature via a 1/8'' (o.d.) PFA line, which is tightly fixed in a meandering cut-out  
35 channel in the aluminum block, covered by an aluminum plate. The entire reactor and the  
36 water lines from and to the thermostat are insulated by Armaflex foam.



37

38 Fig. S1: Left: Turbulent flow photoreactor with thermocouple device for surface temperature  
39 measurements. Right: UV-diode array with power supply,  $1-16 \text{ W m}^{-2}$ ;  $\lambda_{max} = 370 \text{ nm}$ ;  
40  $\Delta\lambda \pm 20 \text{ nm}$  (QUMA-Elektronik & Analytik, Wuppertal).

41 The flow conditions in the reactor are turbulent and not laminar to avoid transport limitations  
42 of the standard ISO method for fast uptake kinetics.<sup>4,5</sup> This is achieved by blowing the gas  
43 mixture via the 6 inlet holes towards a turbulence barrier directly in front of the sample,  
44 forming “lee-wave” turbulences on the sample. In addition, for the present study the distance  
45 between the sample and the window was only 1-2 mm (ISO 5 mm) leading to higher gas  
46 velocities. Since the hand-brushed paint showed also significant surface roughness ( $\sim\pm 0.5$   
47 mm), the turbulent flow conditions were maintained over the whole sample surface without  
48 using additional turbulence barriers, as recommended in Ifang et al..<sup>4</sup> This was verified by  
49 varying the sample/window distance ( $h$ ), for which the uptake is independent of  $h$ , see  
50 equation (I), in the absence of transport limitations. When reducing the reactor volume  
51 (decreasing  $h$ ), the lower reaction time is exactly compensated by the increasing surface to  
52 volume ( $S/V$ ) ratio.

53 In contrast to the original ISO method, which considers zero order kinetics,<sup>3</sup> uptake  
54 coefficients for NO, NO<sub>2</sub> and HONO were calculated assuming first order kinetics:

$$55 \quad (I) \quad \gamma = \frac{4 \cdot \ln\left(\frac{c_{t=0}}{c_t}\right) \cdot \Phi_g}{S \cdot \bar{v}},$$

56 for which  $c_{t=0}$  and  $c_t$  are the mixing ratios [ppb] at the inlet and exit of the photoreactor,  
 57 respectively,  $\Phi_g$  is the gas flow rate [ $\text{cm}^3 \text{s}^{-1}$ ],  $S$  the surface area of the sample [ $\text{cm}^2$ ] and  $\bar{v}$   
 58 the average velocity of the reactants [ $\text{cm s}^{-1}$ ] according to the gas kinetic theory ( $\bar{v} =$   
 59  $(8 \cdot R \cdot T \cdot \pi^{-1} \cdot M^{-1})^{0.5} \cdot 100$ ; with  $R = 8.314 \text{ J mol}^{-1} \text{ K}^{-1}$ ,  $T$ : absolute temperature [K] and  $M$ : molar mass  
 60 [ $\text{kg mol}^{-1}$ ]). First order kinetics was verified by changing the gas flow rate and the  
 61 concentrations of the reactants. In the present study, NO and NO<sub>2</sub> levels only in the range 80-  
 62 150 ppb were applied (for comparison ISO: 1 ppm) for which first order kinetics are fulfilled.<sup>1</sup>  
 63 In the optimized photoreactor, uptake coefficients of at least up to  $\sim 3 \times 10^{-4}$  (or photocatalytic  
 64 deposition velocities of  $v_{\text{photo}} \approx 3 \text{ cm s}^{-1}$ , for definition see ref. <sup>4</sup>) can be determined without  
 65 significant transport limitation of the reactants to the surface.

66 The samples were irradiated by a diode array (QUMA-Elektronik & Analytik, Wuppertal),  
 67 allowing variable UVA irradiance levels between 1-16  $\text{W m}^{-2}$  (see Fig. S1 and Fig. S2). The  
 68 diodes have an intensity maximum  $\lambda_{\text{max}} = 370 \text{ nm}$  ( $\Delta\lambda \pm 20 \text{ nm}$ ), for which almost all emitted  
 69 light intensity falls below the threshold limit wavelength for TiO<sub>2</sub> (Anatas) excitation of <388  
 70 nm. The irradiance was determined via a small planar cosine correcting optical diffuser (Ocean  
 71 Optics CC-3-DA) connected to a diode array mini-spectrometer (Ocean Optics USB 4000). The  
 72 irradiance was averaged over 12 different positions 2 mm behind the Pyrex window (at the  
 73 same distance as the sample) using only the upper cap of the reactor. The Ocean Optics system  
 74 was calibrated by intercomparison with a calibrated spectrophotometer with an electronically  
 75 cooled Charge Coupled Device (CCD) detector (Meteoconsult) for measuring actinic fluxes. For  
 76 the intercomparison a UV/VIS fluorescence bulb at 1 m distance was used, for which the  
 77 cosine correction of the Ocean Optics system is near unity and the irradiance is equal to the  
 78 actinic flux.

### 79 **S3 Analytical Instrumentation**

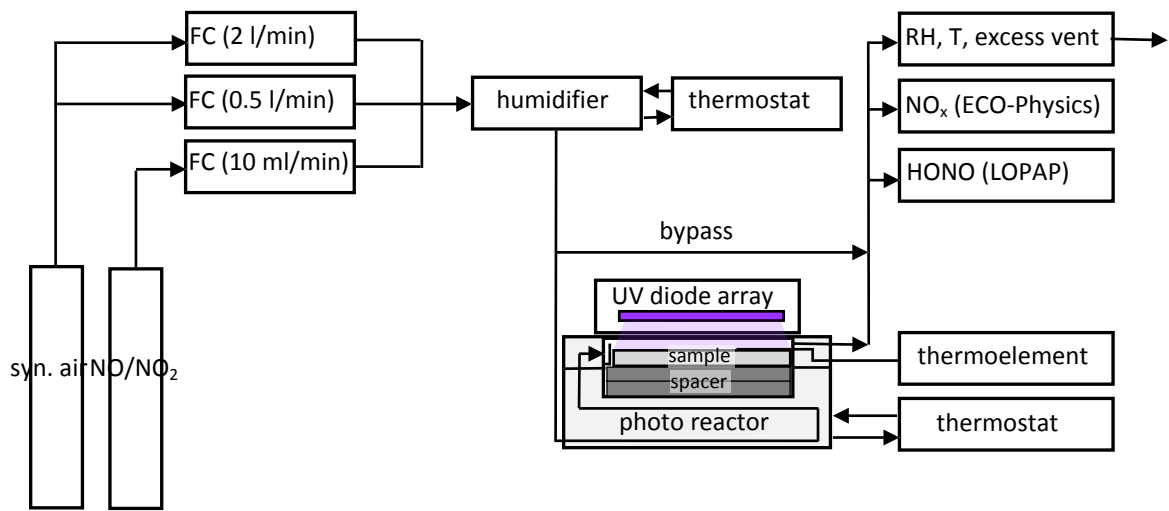
80 Nitrogen oxides (NO<sub>x</sub> = NO + NO<sub>2</sub>) were measured by chemiluminescence detection of NO  
 81 using a molybdenum converter for NO<sub>2</sub> conversion (Eco-Physics CLD 899Y, detection limit: 25  
 82 ppt). The NO<sub>x</sub> channel of the instrument shows quantitative interferences against NO<sub>z</sub> species  
 83 (NO<sub>z</sub> = NO<sub>y</sub>-NO<sub>x</sub>), thus overestimating the NO<sub>2</sub> level.<sup>6</sup> However, since HONO was found to be  
 84 the only significant NO<sub>z</sub> species formed in the photocatalysis of NO<sub>x</sub> on the paint sample,<sup>1</sup> the

85 NO<sub>2</sub> concentration was simply calculated from the difference of the “NO<sub>2</sub>” signal and the  
86 measured HONO level (see below). Both channels of the instrument were calibrated by a  
87 certified NO calibration mixture (Messer, 450 ppb, stated accuracy of ≤5 %). The converter  
88 efficiency for the NO<sub>x</sub> channel of unity (100±1 %) was regularly controlled by an O<sub>3</sub> titration  
89 unit (Ansyco GPT/00).

90 HONO was measured by a sensitive and selective LOPAP instrument (Long Path Absorption  
91 Photometer), which is explained in detail elsewhere<sup>7,8</sup> and which was successfully validated  
92 against the spectroscopic DOAS technique under complex atmospheric and smog chamber  
93 conditions.<sup>9</sup> During the laboratory study the instrument had a detection limit of ~5 ppt for a  
94 time resolution of 3 min.

95 The temperature of the paint surface was measured by a calibrated thermocouple (Omega  
96 Engineering GmbH, Type K, 0.5 mm diameter, accuracy ±0.5 K), while the relative humidity  
97 and the temperature of the reaction mixture behind the reactor were measured by a  
98 calibrated humidity sensor (HYTELOG-USB, Hygrosens Instruments GmbH, accuracy ±2% RH).  
99 The relative humidity on the sample surface in the photoreactor was calculated based on the  
100 absolute humidity, derived from the temperature and relative humidity of the Hygrosens  
101 sensor and the average temperature of the surface during irradiation, using a simple form of  
102 the Clausius Clapeyron relation ( $p(\text{H}_2\text{O}) = 10^{(8.946-2260/T)}$  in [Torr]).

103 **S4 Experimental set-up**



104  
105 Fig. S2: Experimental set-up (FC: flow controller).

## 107 References Supplement

---

- 1 S. Laufs, G. Burgeth, W. Duttlinger, R. Kurtenbach, M. Maban, C. Thomas, P. Wiesen and J. Kleffmann, *Atmos. Environ.*, 2010, **44**, 2341-2349.
- 2 M. Gallus, Diploma Thesis, University of Wuppertal (2011).
- 3 ISO 22197-1. Fine Ceramics (Advanced Ceramics, advanced Technical Ceramics) – Test Method for Air-Purification Performance of Semiconducting Photocatalytic Materials – Part 1: Removal of Nitric Oxide. Reference number ISO 22197-1:2007(E), Switzerland (2007).
- 4 S. Ifang, M. Gallus, S. Liedtke, R. Kurtenbach, P. Wiesen, J. Kleffmann, *Atmos. Environ.*, 2014, **91**, 154-161.
- 5 C. Minero, A. Bedini, M. Minella, *Int. J. Chem. React. Eng.*, 2013, **11(2)**, 717–732.
- 6 G. Villena, I. Bejan, R. Kurtenbach, P. Wiesen, J. Kleffmann, *Atmos. Meas. Tech.*, 2012, **5**, 149-159.
- 7 J. Heland, J. Kleffmann, R. Kurtenbach, P. Wiesen, *Environ. Sci. Technol.*, 2001, **35**, 3207-3212.
- 8 J. Kleffmann, J. Heland, R. Kurtenbach, J. Lörzer, P. Wiesen, *Environ. Sci. Pollut. Res.*, 2002, **9 (special issue 4)**, 48-54.
- 9 J. Kleffmann, J. C. Lörzer, P. Wiesen, C. Kern, S. Trick, R. Volkamer, M. Rodenas, K. Wirtz, *Atmos. Environ.*, 2006, **40**, 3640-3652.